INFN/TC-98/18
17 Luglio 1998

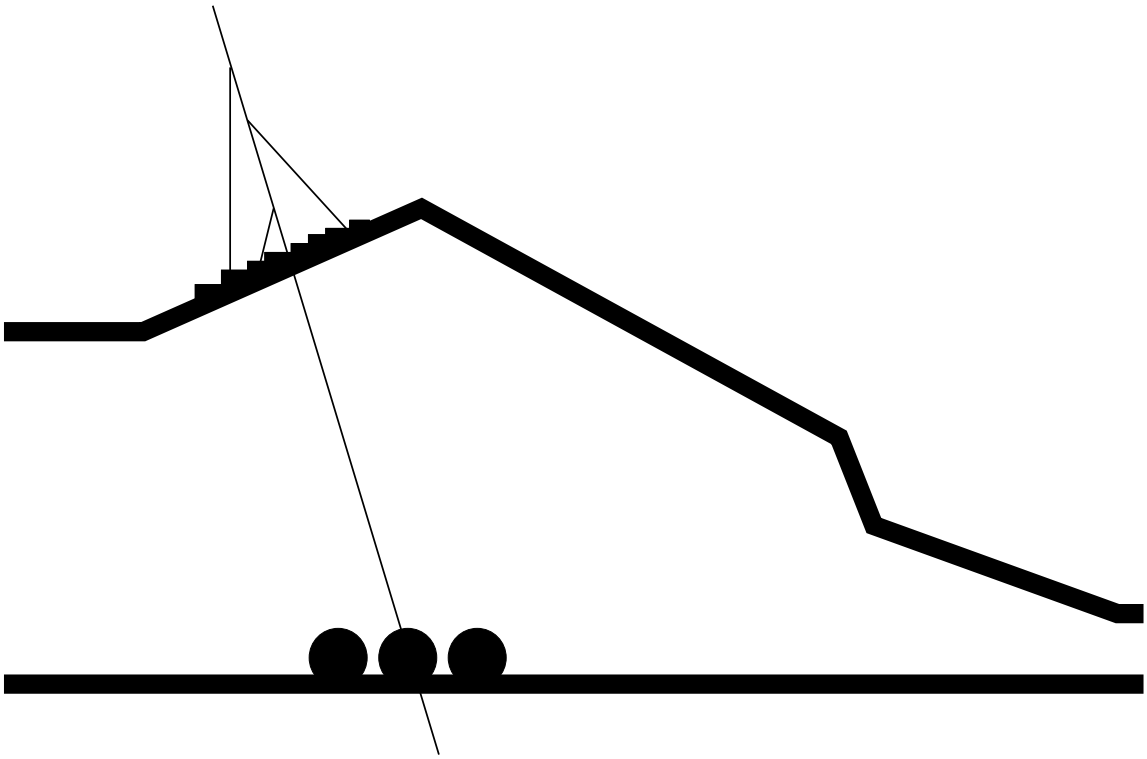

Methods for precise photoelectron counting with photomultipliers

Roberto Dossi[a], Aldo Ianni[a], Gioacchino Ranucci[b], Oleg Ju. Smirnov[c],

INFN - Laboratori Nazionali del Gran Sasso

Published by **SIS-Pubblicazioni**
dei Laboratori Nazionali di Frascati

INFN - Istituto Nazionale di Fisica Nucleare
Laboratori Nazionali del Gran Sasso

INFN/TC-98/18
17 Luglio 1998

Methods for precise photoelectron counting with photomultipliers

Roberto Dossi[a], Aldo Ianni[a], Gioacchino Ranucci[b], Oleg Ju. Smirnov[c],

[a] *LNGS and University of L'Aquila, Physics Department - Italy*
[b] *Sezione INFN Milano, Via Celoria, Milano - Italy*
[c] *Joint Inst. for Nuclear Research, Dubna - Russia*

Abstract

A series of measurements has been performed on a THORN EMI 9351 phototube in order to investigate its response to a low light intensity. Precise procedures to determine the intensity of the incident photon flux have been developed and compared. The data show that the various approaches give consistent and reliable results, thus allowing the precise calibration of the device for applications of photon counting.

1 Introduction

In many experimental conditions involving scintillators and photomultipliers the light pulse arriving at the photocathode contains very few photons. The mean value μ of the Poisson distributed number of photoelectrons (p.e.) detected in a burst depends on various factors. The most important factors being the energy of the incident particle in the scintillator, the geometrical coverage of the photocathode, and the quantum and collection efficiency of the phototube. In a given experiment the precise evaluation of μ can be accomplished with different methods, based on the use of the information contained in the output of the phototube.

In the present paper we present the results of an investigation carried out to evaluate and compare different methods of mean p.e. number estimation from the PMT charge distribution. We studied the charge distribution of the Thorn EMI 9351 PMT planned for use in the Borexino experiment. In Borexino an organic liquid scintillator is used to detect the ^7Be solar neutrinos through the electron-neutrino elastic scattering. A rate of few p.e. per PMT is expected (for a reference on Borexino see for example [10, 11]).

In order to study the response of the PMT for various levels of a light intensity we used optical filters (that do not change the spectral characteristic of the radiation). These are used to control the amount of the incident light in different measurements.

In table 1 the properties of the filters used are summarized. Here $\tau = \frac{\Phi_T}{\Phi_0}$ is the ratio of the transmitted to the incident luminous flux and D=$\log \frac{1}{\tau}$ is the öptical density¨.

The results of our experiment are described below. In Sec. 2 we underline the features of the PMT charge signal, that are important for the development of a PMT charge response model. In Sec. 3 we discuss the model of the Single Electron Response (SER). In Sec. 4 we present different methods of mean number of p.e. evaluation and in Sec. 5 we analyze the measurements. Sec. 6 contains the conclusions.

2 The PMT charge response to a low intensity light source

The charge response of the PMTs to low intensity light has been studied using the Borexino PMT test facility at the Gran Sasso Laboratories. The experimental set-up is shown in figure 1. A Hamamatsu pulsed laser (0.39mW peak power, 27.3ps pulse width, 415nm wavelength, which is close to the maximum quantum efficiency of PMT 9351) is used to study the PMT charge spectrum. Using the laser internal trigger, an ADC gate is generated, as shown in the same figure. The light pulse from the laser is delivered by a 6 meter long optic fiber into the dark-room. Between the fiber and the PMT, an optical filter support is placed. The dark noise spectrum has also been studied with the laser turned off using the ADC to gate the PMT signal (discriminated at the level of 0.05-0.10 p.e.) in order to cut the electronics noise.

We have performed a set of measurements with different filters using the same PMT. The PMT is placed inside a μ-metal shield in order to screen the Earth's Magnetic field.

Table 1: Properties of the optical filters

Density D	**Transmission τ**	**τ tolerance**
0.3	0.5	5%
0.7	0.2	5%
1	0.1	5%
1.3	0.05	10%
1.7	0.02	10%
2	0.01	10%
3	0.001	20%

The first step of the procedure to determine the mean number of detected photoelectrons requires the precise determination of the single electron response of the phototube.

Assuming that a Poisson distribution describes the p.e. number leaving the photocathode as reported in [2], one can write:

$$\frac{P(2)}{P(1)} = \frac{\mu}{2}, \tag{2}$$

where P(2) and P(1) are the probability to detect two or one p.e. respectively and μ is the mean value of p.e.'s. Therefore, in order to keep the PMT charge multiphotoelectrons responses at the 1% level it is necessary to have $\mu \leq 0.02$. Taking the PMT charge spectrum, we controlled this number using the probability to have zero p.e.:

$$P(0) = \frac{N_{ped}}{N_{trig}} = e^{-\mu}, \tag{3}$$

where N_{ped} is the number of events in the pedestal (i.e. the response when no p.e. leaves the photocathode) and N_{trig} is the number of laser triggers.

For small μ the output of the PMT could be altered by the dark noise of the PMT, which is of the order of some KHz. Because of the dark noise a number of random coincidences can be detected, expressed by:

$$f_{random} = f_{dark} \cdot f_{trig} \cdot \tau_{gate}, \tag{4}$$

where f_{random} is the random coincidence rate, f_{dark} is the dark noise rate and τ_{gate} is the ADC gate. On the other hand for small μ the event rate is, using (3):

$$f_{events} = (1 - P(0)) \cdot f_{trig} \simeq \mu \cdot f_{trig} \tag{5}$$

Therefore, in order to have the random coincidences' contribution at the level of 1% it is necessary to keep:

$$\mu \geq \frac{f_{dark} \cdot \tau_{gate}}{0.01} \tag{6}$$

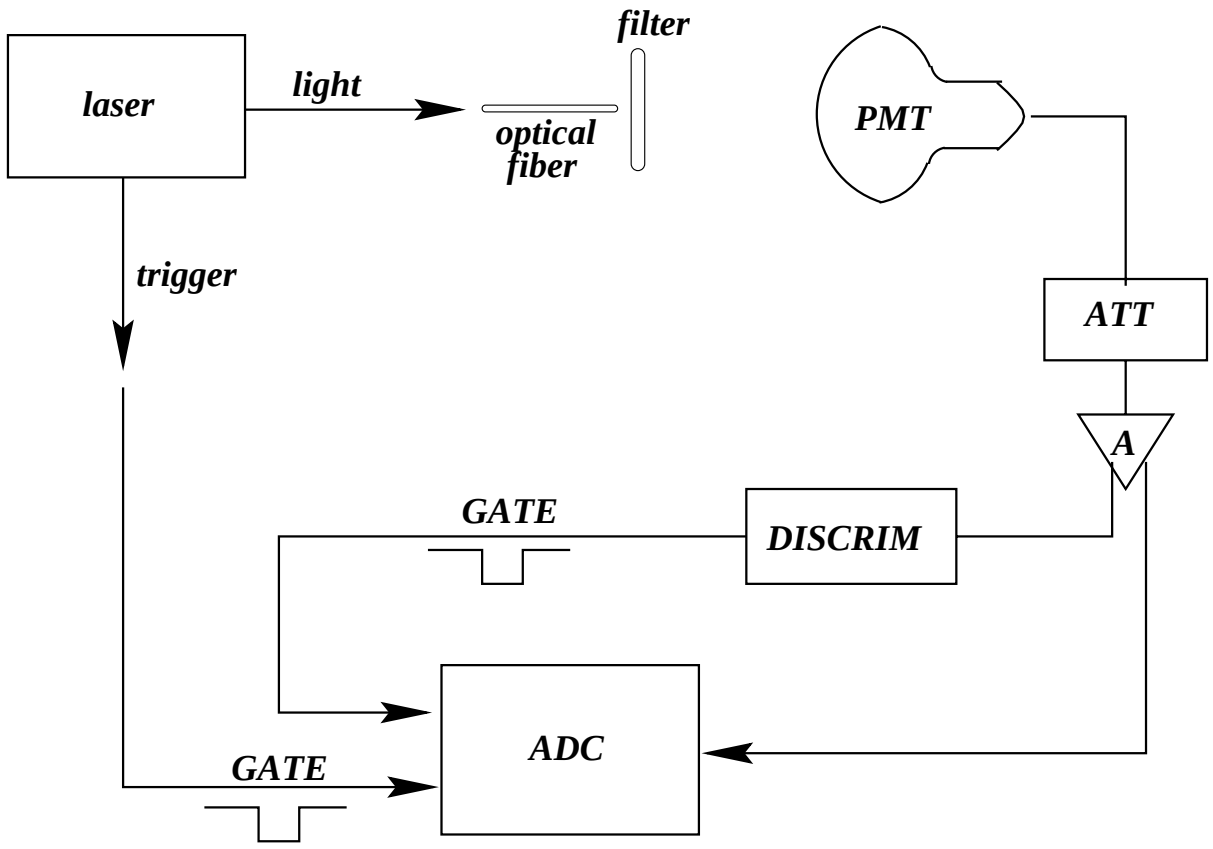

Figure 1: *Sketch of the experimental set-up*

For a 2KHz dark rate and $\tau_{gate} = 80$ns, eqn. (6) gives $\mu \geq 0.016$. Thus, for for $\mu = 0.02$ or greater a PMT response has both a negligible contribution from the dark noise spectrum and of the multiphotoelectrons one.

In figure 2, we show a typical PMT charge spectrum together with the dark noise spectrum from the same PMT. For these data, a software threshold was set at the level of 0.15 p.e. Looking at the two spectra we can point out the following differences: a longer tail and a higher contribution of small amplitude pulses distinguish the dark noise spectrum. The origin of the longer tail events is due to Čerenkov light of cosmic ray particles and scintillation caused by natural radioactivity contamination in the PMT itself, as reported in [3]. In order to understand the origin of the higher contribution of small amplitude pulses we grounded the first dynode and kept the photocathode at a small positive potential. In this way the possible noise from the dynode system was measured.

The spectrum we obtain is also presented in figure 2. It does not fit the difference between the spectra. The most probable origin of this difference is the thermoionic emission from the photocathode material (SbCsK) which is covering the inner parts of the PMT due to the manufacturing procedure of the photocathode. Another contribution, as reported in [4, 5], could come from the elastically scattered and backscattered electrons from the first dynode.

From the consideration above, we note the following:

- a significant amount of small amplitude pulses in the charge spectra is an intrinsic property of the EMI 9135 PMT, and it should be taken into account when modeling the SER;
- a significant difference between the SER and the dark-noise makes it impossible to use the latter distribution for the precise PMT calibration;
- the response of the PMT for a low intensity light source is not a pure SER as, due to the statistical nature of the light counting, there is always a certain amount of multiple p.e. counting with a total probability $1 - P(0) - P(1)$, where $P(0)$ is the probability of no response and $P(1)$ is the probability of a SER.

3 The SER charge spectrum parameters

As it has been mentioned in the previous section, even for small μ, the PMT charge spectrum is not a pure SER. In order to extract the SER spectrum, i.e. the ideal PMT response to one p.e. hitting the first dynode, the pedestal and multiple p.e. response should be rejected from the experimental charge spectrum. We do it using an ideal SER model which is discussed in this section.

The main parameters of the ideal SER we are evaluating in this section are the mean value x_1 of the ideal SER itself and its relative variance $v_1 = (\sigma_1/x_1)^2$, where σ_1 is the ideal SER standard deviation.

3.1 The SER model and fitting function for the PMT response to small μ

An ideal SER model consisting of a gaussian and an exponential is used:

$$SER_0(x) = \begin{cases} \frac{p_E}{A} e^{-\frac{x-x_p}{A}} + \frac{1}{\sqrt{2\pi}\sigma_0} \frac{1-p_E}{g_N} e^{-\frac{1}{2}(\frac{x-x_0-x_p}{\sigma_0})^2} & x > 0 \\ 0 & x \leq 0 \end{cases} \tag{7}$$

with the following parameters:
- A is the slope of the exponential part of the $SER_0(x)$
- p_E is the fraction of events under the exponential function,
- x_p is the pedestal position,

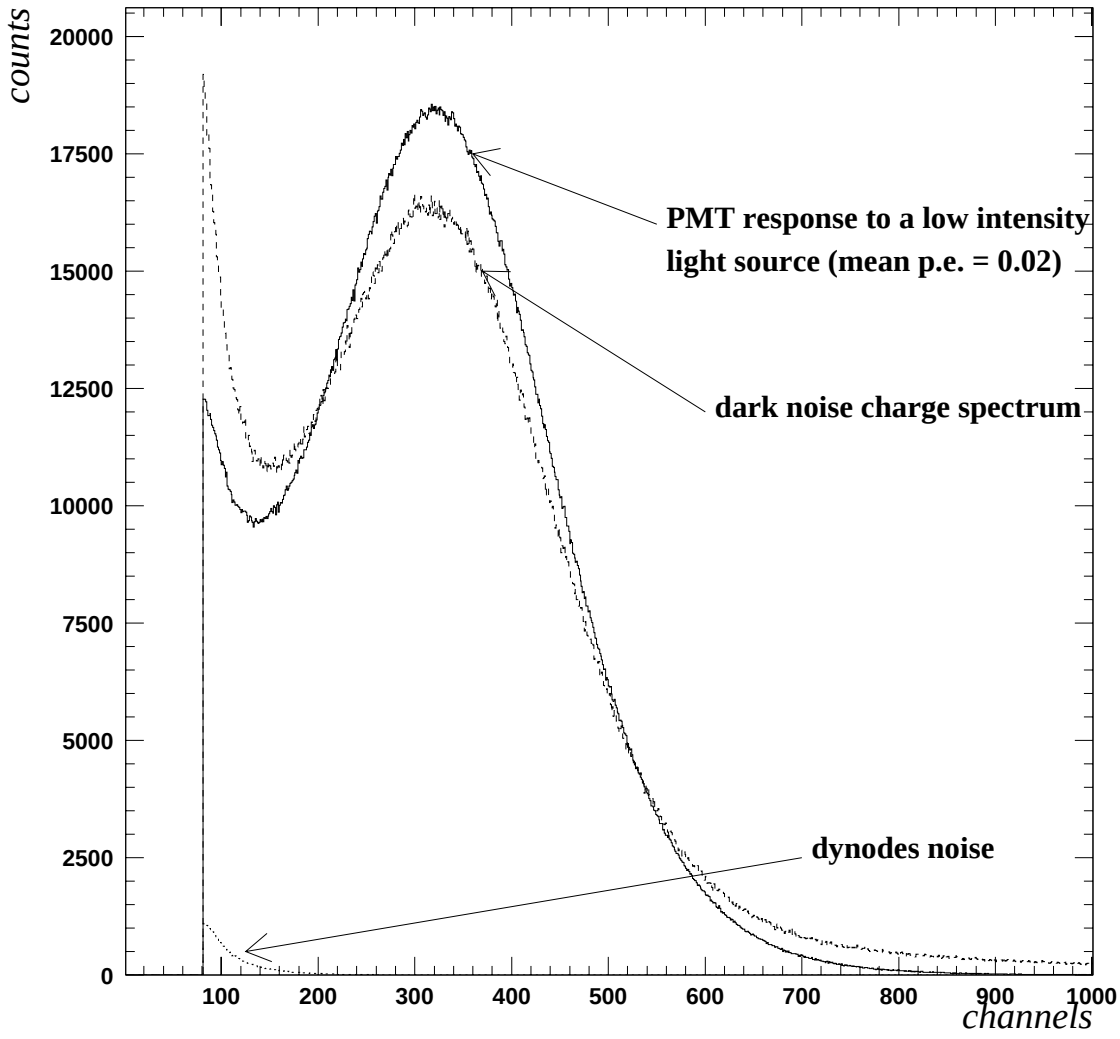

Figure 2: *Dark noise and PMT response to a low intensity light source. The dynodes noise spectrum is also shown*

- x_0 and σ_0 the mean value and the standard deviation of the gaussian part of the single p.e. response respectively;

and the factor

$$g_N = \frac{1}{2}\left(1 + Erf\left(\frac{x_0}{\sqrt{2}\sigma}\right)\right),$$

where $Erf(x)$ is the error function, takes account for the cut of the PMT response gaussian part.

The model has been applied to a number of different PMTs. From this, we find a good quality of the final fit and this justify our choice of the $SER_0(x)$ function.

To account for the electronics noise, we perform a convolution of the ideal SER with a noise function, $Noise(x)$:

$$SER(x) = SER_0(x) \otimes Noise(x), \tag{8}$$

where:

$$Noise(x) = \frac{1}{\sqrt{2\pi}\sigma_p} e^{-\frac{1}{2}(\frac{x-x_p}{\sigma_p})^2}, \tag{9}$$

which fits the pedestal with a proper normalization. The convolution does not influence the gaussian part of the SER since $\sigma_1 >> \sigma_p$ (in our measurements $\sigma_p \sim 0.01\sigma_1$), but it does affect the exponential part because it is closer to the pedestal. The analytical formula for the convolution of the exponential function with the gaussian gives:

$$Ser(x) = \frac{p_E}{2A} \cdot e^{\frac{\sigma_p^2 - 2A(x-x_p)}{2A^2}} \cdot \left(1 + Erf\left(\frac{Ax_p - \sigma_p^2}{\sqrt{2}A\sigma_p}\right)\right). \tag{10}$$

The PMT response for a low light intensity contains a certain amount of multiple primary p.e. signals. Assuming that the PMT response is linear, we can write: $x_n = nx_1$ and $\sigma_n = \sqrt{n}\sigma_1$, where x_n and σ_n are the mean value and the standard deviation of the PMT response to n-p.e., respectively. Taking into account the Poisson distribution of the detected light and using a gaussian approximation for the responses to $np.e. > 2$ (the validity of this assumption is discussed later), the multi-p.e. response will have the following form:

$$M(x) = \sum_{n=2}^{N_M} \frac{P(n;\mu)}{\sqrt{2n\pi}\sigma_1} e^{-\frac{1}{2n}\left(\frac{x-nx_1-x_p}{\sigma_1}\right)^2} \tag{11}$$

where the response to n p.e. is approximated by a gaussian and $P(n;\mu)$ is the Poisson distribution with mean value μ to account for the different contributions of $0 \to n$ p.e. In eq. (11) N_M, the maximum number of multiple-p.e. responses considered, depends on μ and on the ADC scale. The function $M(x)$ has three additional parameters μ, x_1 and σ_1.

For fitting the PMT response to a low intensity light source (small μ) with a small contribution of multiple-p.e., approximate values of x_1 and σ_1 can be used:

$$x_1 \approx (1 - p_E) \cdot x_0 + p_E A \tag{12}$$

$$\sigma_1 \approx (1 - p_E) \cdot (\sigma_0^2 + x_0^2) + 2p_E A^2 - x_1^2. \tag{13}$$

The approximate character of these formulae come from the cut in the gaussian part of the SER, whose portion below 0 is truncated.

A more complex analytical approach has been developped for larger μ with lower statistics data. This approach gives a precise value of x_1 and σ_1 (see appendix A). Here we are following the standard procedure of the SER definition described in literature [9], making corrections for the multiple hits and small amplitude pulses contribution.

From eqs. (8), (9) and (11) the fitting function for the PMT spectrum can be written as:

$$f(x) = N_0 \cdot (P(0) \cdot Noise(x) + P(1) \cdot SER(x) + M(x)) \tag{14}$$

where N_0 is a normalization factor. In eq. (11) we choose the values of x_0, σ_0, p_E and A as free parameters for fitting. When used with small μ, this function will work well only for very high statistics because of the larger magnitude ot the $P(0)$ probability.

We should point out that eq. (14) was used only to separate the contribution of small amplitude pulses from the events in the pedestal and can be applied only in the case of small μ (~ 0.02) and high statistics data. For 1% precision of μ definition at 1σ C.L. the necessary statistics is 10^5 (see appendix B). We verified the statistics needed for a 1% precision of the SER parameters definition is of the order of 10^5 excluding the pedestal. So for $\mu \sim 0.02$ the total number of events should be 10^5.

3.2 The SER charge spectrum parameters

To obtain the SER parameters x_1 and v_1 the following procedure has been applied.

1. Using eq. (3) an approximate value of μ is defined by evaluating the ratio of the events under the gaussian fitting the pedestal to the total number of triggers.

2. The fit of the experimental data with eq. (14) is performed with fixed μ (see figure (3)).

3. The mean value, x_m^*, and the r.m.s., σ_m^*, have been defined for the experimental spectrum after the pedestal rejection. To reject the pedestal events the experimental data have been used for $x > x_p + 5 \cdot \sigma_p$, while the data have been replaced by the fitting curve (see black-painted area in figure 4) for $x < x_p + 5 \cdot \sigma_p$.

4. The number of pedestal events have been estimated from the difference between the total number of triggers and the events under the modeling curve (see figure 4), then the precise μ value has been obtained using (3).

5. x_1 and v_1 (the SER relative variance) have been obtained from x_m^* and $v_m^* = (\sigma_m^*/x_m^*)^2$ (the PMT charge spectrum relative variance) discarding the contribution of the multiple-hits, using the formulae (see appendix C):

$$x_1 = x_m^* \left(1 - \frac{\mu}{2}\right) \tag{15}$$

$$v_1 = \frac{v_m^* - \frac{\mu}{2}}{1 - \frac{\mu}{2}} \tag{16}$$

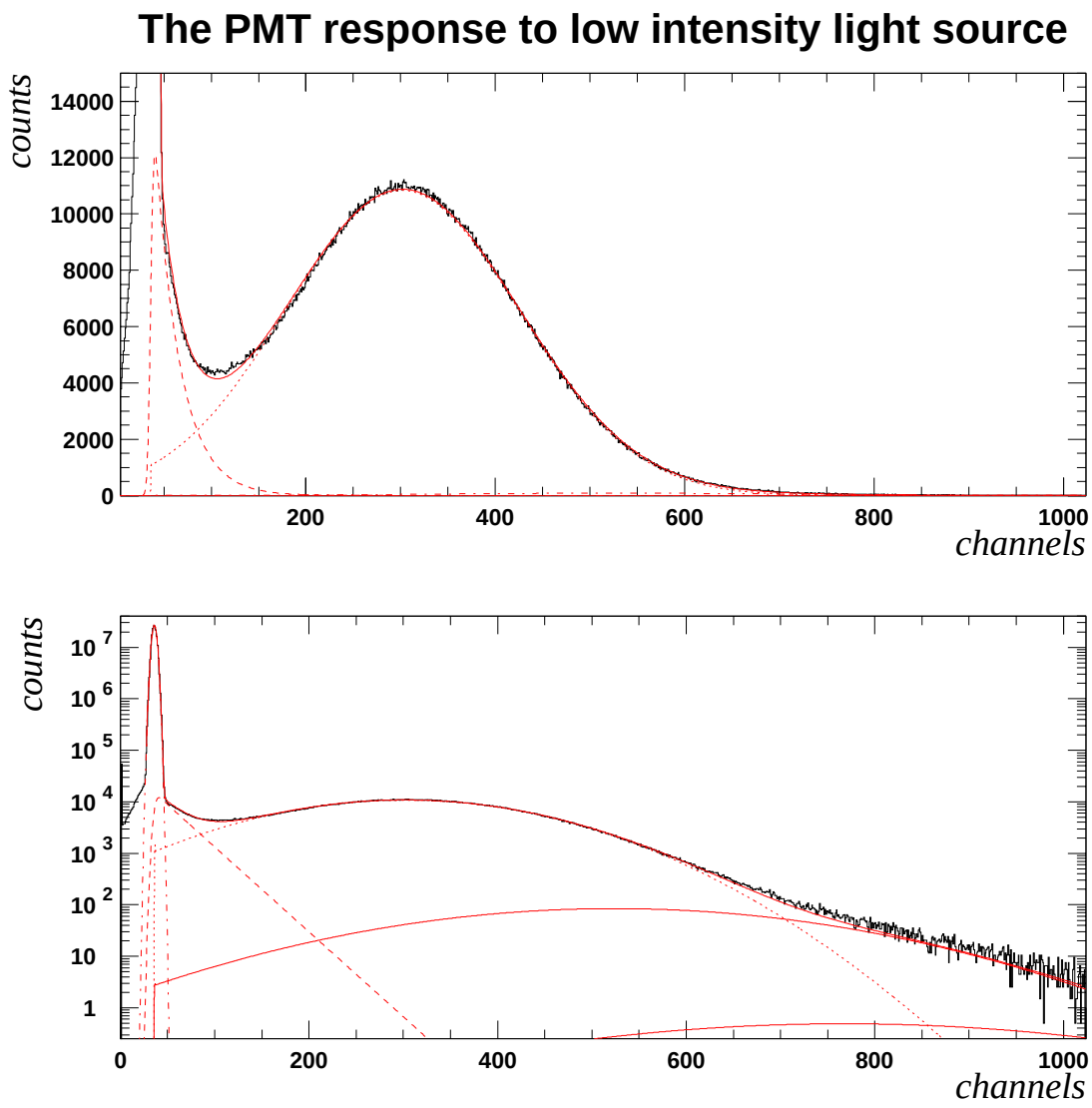

Figure 3: *The SER charge spectrum taken with a mean p.e. number equal to 0.021. In the upper plot the exponential part and the gaussian one in the SER are shown. The exponential function is convoluted with the noise. The contribution of 2 and 3 p.e. to the PMT response can be seen in the logarithmic scale.*

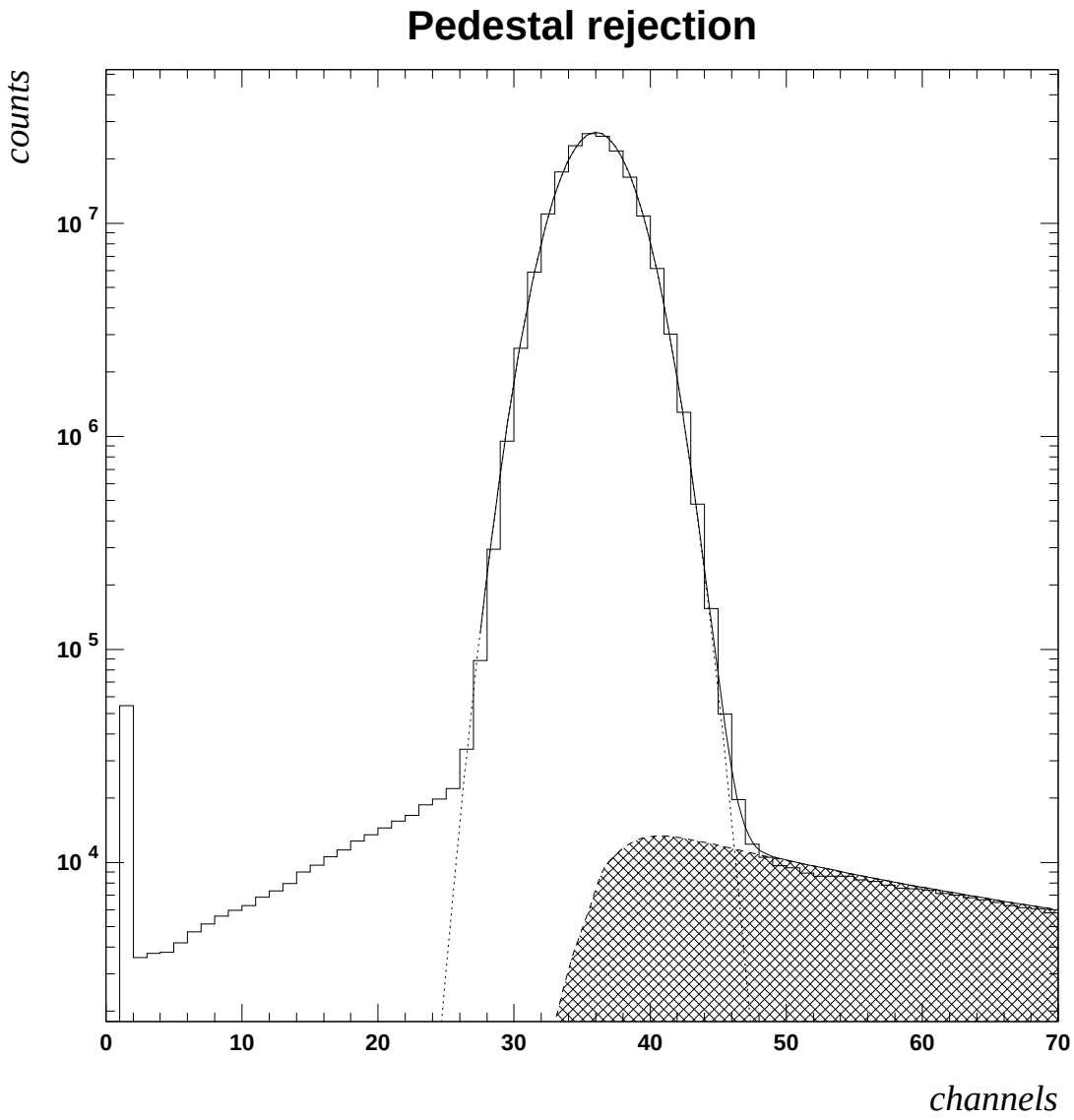

Figure 4: *The pedestal rejection procedure using the single photoelectron fitting function. The SER model function convoluted with the noise circumscribe the black-painted area.*

4 Estimation of the mean number of p.e.

We studied four different procedures to obtain the mean p.e. number from the PMT charge spectrum.

1. We assume the Poisson distribution of the detected light, the mean p.e. number can be defined from (3):
$$\mu = -ln(P(0)).$$

2. In addition, we assume the linearity of the PMT, the electronics and the ADC; then the mean number of p.e. can be estimated from the mean value of the charge spectra using the calibration of the SER:
$$\mu = \frac{x_m}{x_1}, \tag{17}$$
where
$$x_m = \frac{\sum N(i) \cdot i}{\sum N(i)}, \tag{18}$$
and it is defined for all spectra, including pedestal, being N(i) the charge response to the i-th photoelectron. It is interesting to note that x_1 is different (lower) than the location of the peak in the output charge spectrum for single photoelectron.

3. The mean p.e. number can be estimated from the relative variance of the charge spectra. For the assumption involved see references [2, 6]. If v_1 is the relative variance of the SER spectrum, then:
$$v = \left(\frac{\sigma_m}{x_m}\right)^2 = \frac{1 + v_1}{\mu},$$
i.e.
$$\mu = \frac{1 + v_1}{v}. \tag{19}$$

4. Supposing, as before, the linearity of the PMT response and the mutual independence of every primary p.e. participating in the anode charge formation , one can construct the basis set of functions $f_N(x)$, which can be used for the charge distribution fitting:
$$f_N(x) = f_{N-1}(x) \otimes f_1(x), \tag{20}$$
where $f_N(x)$ is the response of the PMT for N-p.e. and $f_1(x)$ is the SER in (7). The parameters in $f_1(x)$ have to be defined with the procedure described in section 3. Taking into account the underlined assumptions, the fitting function for a measured charge spectrum can be written as:
$$f(x) = \sum_{N=1}^{N_{max}} P(N) f_N(x) + P(0) f_p(x), \tag{21}$$

Table 2: Mean photoelectrons number obtained implementing differents methods#,##.

No	τ	Att(dB)	$\mu = x_m/x_1$	$\mu = -ln(P(0))$	$\mu = (v_1+1)/(v-v(p))$	fitI(χ^2)
1	0.001	0	0.0211	0.0211	0.0211	#
2	0.01	10	0.202	0.208	0.204	0.206(2.72)
3	0.02	10	0.432	0.436	0.431	0.430(1.48)
4	0.05	10	1.10	1.07	1.09	1.08(2.42)
5	0.1	10	2.12	2.06	2.10	2.10(1.69)
6	0.2	10	4.16	#	4.20	4.12(1.25)
7	0.5	20	10.2	#	10.2	10.13(2.14)
8	##	20	21.7	#	21.7	21.3(1.65)

too low statistics for the method used.

no filters

where $P(N)$ is the Poisson distribution of N and $f_p(x)$ is the noise function. For μ big enough instead of (20) a gaussian approximation can be used. In this case, as we show below, the functions $f_N(x)$ can be gaussians. This is practically the case of (14).

5 Data analysis

The data analysis of the measurements taken with different filters have been performed using the four methods mentioned above. The results of the analysis are presented in table 2 and discussed in the next subsections.

We aimed to achieve 1% accuracy in our measurements, so we keep significant numbers for all the data in table 2 at this level of accuracy. We estimated the accuracy only for the $P(0)$ method (see appendix B) directly. It is difficult to estimate the precision of the other methods in such a direct way but one can see from table 2 that the different methods give equal results within the claimed accuracy.

5.1 The SER parameters

In order to obtain with a satisfactory precision the SER parameters a high statistics data sample of $1.8 \cdot 10^8$ laser trigger was taken with an optical filtet having $\tau = 0.001$. Using the procedure described above, we obtained the following numbers.

1. The number of events under the SER histogram after pedestal rejection was $N_{ev} =$

Table 3: *PMT charge spectrum parameters (left column) and the SER ones (right column).*

x_m=249.4	x_1=246.7
v=0.303	v_1=0.296

$3.725 \cdot 10^6$. The mean number of photoelectrons was calculated to be:

$$\mu = -ln\left(1 - \frac{3.725 \cdot 10^6}{1.8 \cdot 10^8}\right) = 0.021,$$

since $N_{ev} = N_{triggers}(1 - P(0))$.

2. With μ fixed to 0.021 the fit has been performed with the function of eq. (14) (see figure 3).

3. The calculated PMT charge spectrum parameters are reported in table 3.

4. Using the fit, the pedestal events number have been estimated, leading to the precise evaluation of the number of p.e., which however resulted virtually unchanged (indeed the new evaluation turns out to be 0.0211). It can be seen in the figure 4 that we have a certain amount of negative small amplitude pulses near x_p. These signals are registered when the trigger hits just after the big amplitude dark event pulse (which has negative overshoot) has occurred. These pulses should be considered as no-p.e. events.

5. The SER parameters obtained from eqs. (15-16) are presented in table 3. From which it can be resumed that the difference with the parameters inferred directly by the "not corrected" charge spectrum is negligible.

5.2 The attenuator calibration

In order to increase the dynamical range of the ADC an attenuator has been used before the amplifier as shown in figure 1. Using a precise charge generator (LeCroy mod. 1976) the calibration of the ADC for the attenuator set at 0, 10, 20 and 30dB respectively has been performed. For every set of data a linear fit has been done. The pedestal, measured with high statistics, has been taken as the constant parameter of the fitting linear function. Finally, the calibration of the attenuator has been obtained as the ratio of the corresponding slopes. The data are presented in table 4.

5.3 "No photoelectron event number" estimation

Together with the pedestal rejection procedure described in subsection 3.2 (first column in table 5), two alternative methods have been tried.

Table 4: *Attenuator calibration parameters*

setting	attenuation
10dB	3.20
20dB	10.24
30dB	33.49

Table 5: Mean p.e. number evaluated by three different methods of pedestal rejection. I method: using the single photoelectron response fitting function to discard real photoelectrons small amplitude pulses. II method: using a suitable cut (see text) to discard real pulses from the pedestal region. III method: fitting the pedestal events with a gaussian.

No	**I method**	**II method**	**III method**
1	0.0211	0.0212	0.0202
2	0.208	0.207	0.205
3	0.431	0.433	0.425
4	1.29	1.32	1.30

1. We fixed a value averaging the SER around $x_p + 5\sigma_p$ with a spread of $\pm\sigma_p$, then we rejected the events under the measured charge spectrum for $x > x_p + 5\sigma_p$ plus the events under the rectangular area from x_p up to $x_p + 5\sigma_p$. The mean p.e. number for different measurements are listed in table 5 in the second column.

2. Fitting the pedestal with a Gaussian, we took as pedestal events the normalization factor N_{ped}. The mean p.e. number, obtained with this method of pedestal rejection, for different measurements are listed in table 5 in the third column.

The first method gives better results evaluating the pedestal. Nevertheless the second one, easier to implement, gives results in acceptable agreement in comparison with the former.

5.4 Mean photoelectrons number estimation using SER mean value

Having evaluated x_1 (the mean value of the SER) one can estimate μ from (17). Data are presented in table 2.

We should note that, because of the asymmetrical shape of the SER, x_1 is less than x_0, the main peak position. For a sample of 40 PMTs tested during the preparation of the C.T.F. this difference was in the range of 0-15%. So it is not correct to calibrate the PMTs using x_0.

Here we would like also to point out another difficulty that arises from the non-equivalence of x_0 and x_1. Not knowing apriori the x_1 value which should be defined in the complicated enough way described before we adjust the PMT operating high voltage in order to have the gain factor at $k = 10^7$ at the peak position. It means that the real PMT gain is up to 15% less and is equal to $k' = kx_1/x_0$.

5.5 The basis set of the fitting functions

5.5.1 Convolution of the ideal PMT response

A fitting function for the measured charge spectra can be obtained from the known SER_0 function ($f_1(x)$). The SER_0 parameters was obtained by fitting high statistics data. Then the set of discrete functions have been obtained as recursive convolution:

$$f_N^0(i) = \sum_{k=1}^{i} f_1^0(k) \cdot f_{N-1}^0(i-k). \tag{22}$$

Such a set f_N^0 has been obtained for every attenuator setting. In figure (5) and (6) we show these functions (continuous line) evaluated for 0 and 30dB respectively. Then the convolution with the gaussian noise function has been performed:

$$f_N(i) = \sum_{k=i-10\sigma_p}^{i+10\sigma_p} f_N^0(k) \cdot Noise(i-k). \tag{23}$$

So the final fitting function is:

$$f(i) = N_0(\sum_{N=1}^{N_{max}} P(N) f_N(i) + P(0) f_p(i)). \tag{24}$$

The data with $\mu \leq 4$ were fitted with four free parameters: the normalization N_0, the mean number of p.e. μ, x_p and σ_p. For $\mu > 4$ when events in pedestal cannot be clearly separated x_p and σ_p were fixed at the measured values. In table 2 we present in the last column the values of μ and χ^2 obtained using (24).

An example of this fitting method is presented in figure 7.

5.5.2 Gaussian approximation of basic functions f_N

For large μ (> 4) a gaussian approximation has been tried instead of using the function (24). In this case instead of (23) we use:

$$f_N(x) = \frac{1}{\sqrt{2\pi}\sigma_N} e^{-\frac{1}{2}\left(\frac{x-x_N}{\sigma_N}\right)^2}, \tag{25}$$

with:

$$x_N = \frac{x_1 N}{k_{att}}, \tag{26}$$

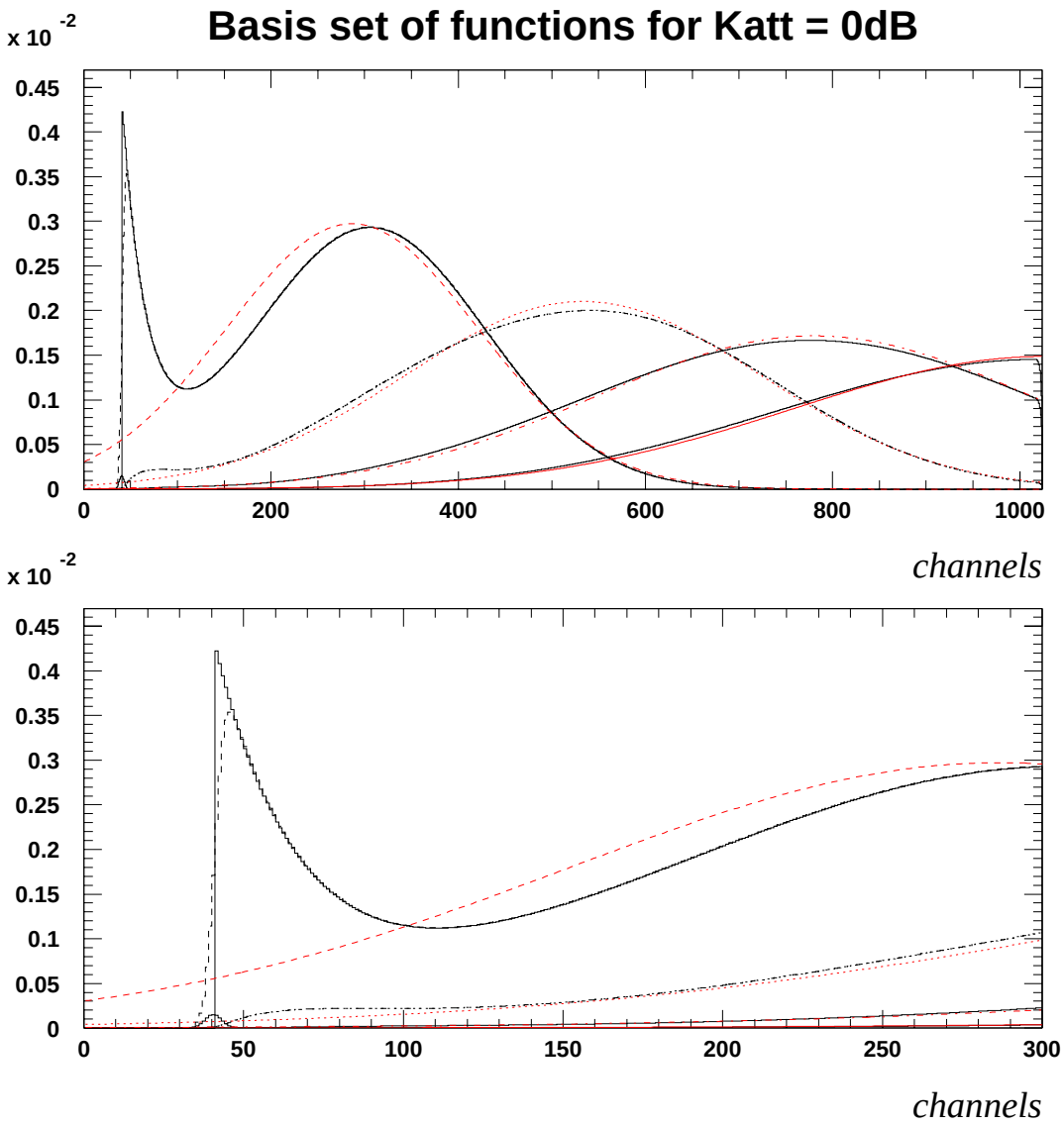

Figure 5: *Set of convoluted and gaussian (dashed lines) functions to work out the phototube charge spectrum fitting for a 0dB attenuator setting.*

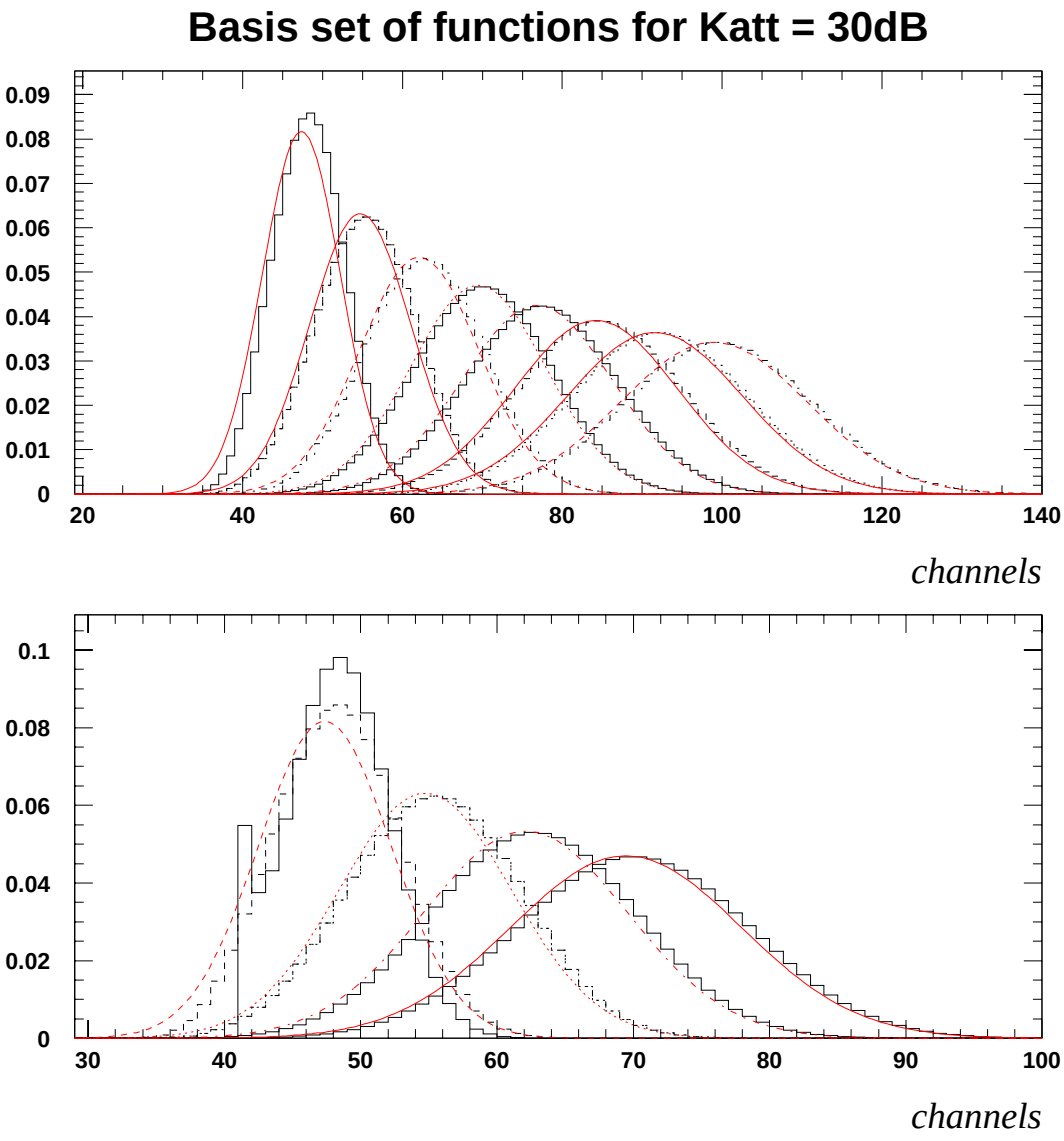

Figure 6: *As in figure (5) but for a 30dB attenuator setting.*

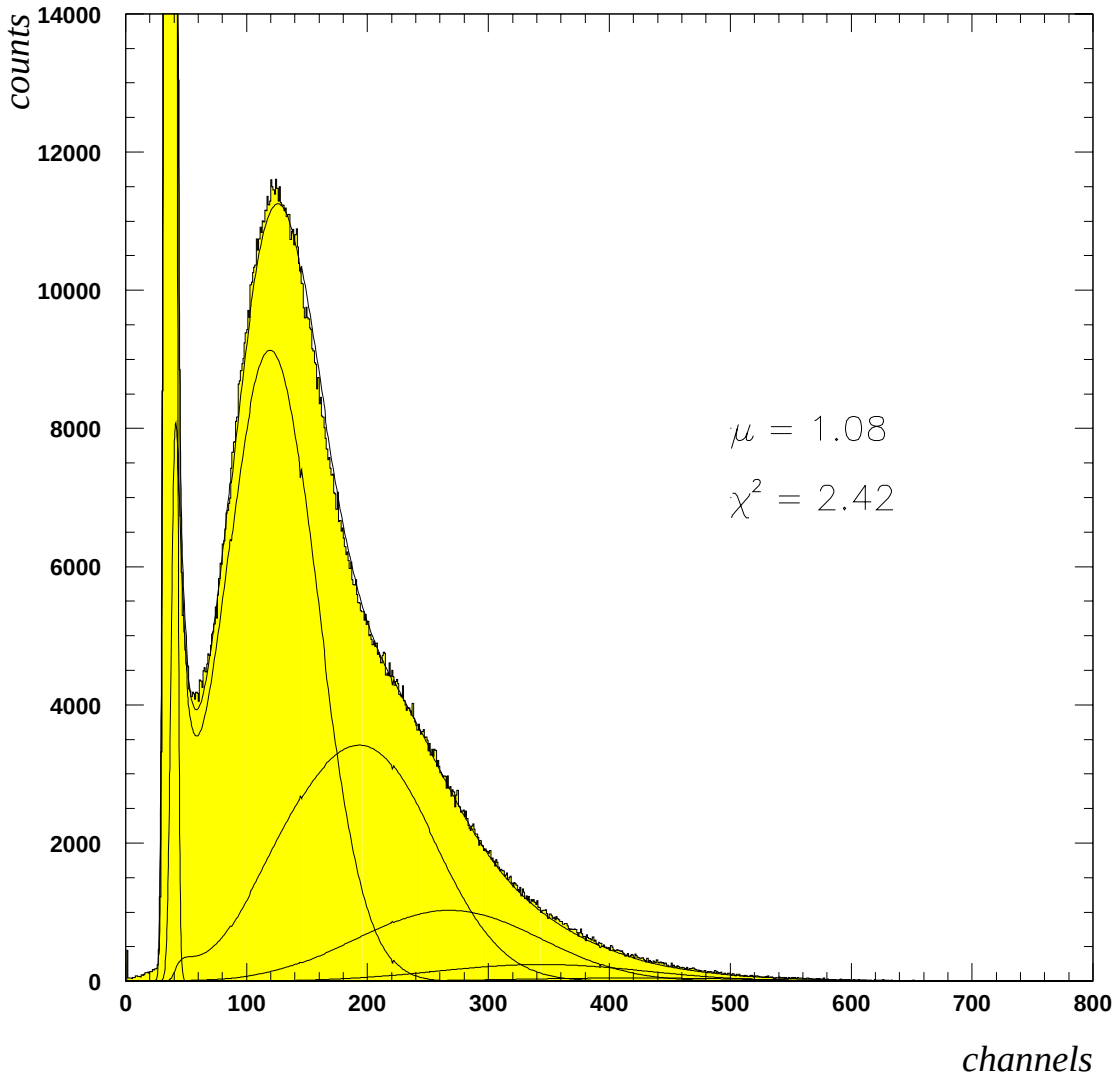

Figure 7: *PMT charge spectrum fit using the convolution method*

$$\sigma_N^2 = N(\frac{\sigma_1}{k_{att}}) + \sigma_p^2. \tag{27}$$

In figures 5 and 6 we plot these gaussians (dashed lines) for comparison with eq.(23). It can be seen that for a number of p.e. ≥ 3 the gaussian coincides with the corresponding function from eq. (23). One can also see (figure 6) that the noise significantly changes the f_N functions for high k_{att}, so even the SER can be replaced by a gaussian in a noisy enviroment.

For $0.05 < \mu < 1$ a combined method has been used: as $f_1(x)$ was chosen the SER function and for each $f_N(x)$ $(N > 1)$ were chosen gaussians as in (25).

An example of this fitting method is presented in figure 9 (lower plot).

5.6 The quality of the fit

The quality of the fit was checked by three criteria:

1. χ^2 method;

2. comparison with the μ value obtained by the other methods;

3. the μ value obtained for the different attenuator setting should be the same.

The convolution method is good for $\mu \geq 0.05$ and up to $\mu \simeq 10$ then it gives slightly smaller values due to the accumulated errors while constructing the f_N functions. The gaussian approximation gives good results starting from $\mu > 1$ (even if χ^2 is big), and it is definitely better for high μ values ($\mu > 10$). For $0.05 < \mu < 1$ the combined method gives results comparable with the convolution one.

5.7 Estimation of μ using the relative variance

Estimation of μ using formula (19) for $\mu > 4$ gives significantly different values in comparison with the other methods used (see table 6). A possible reason could be the fluctuations in the electron collection, electrons transfer efficiency etc. In the case of a normal distribution (it is also true for a Poisson distribution) of the emitted light one can take into account such fluctuations, as reported in ref. [6]:

$$v = v(p) + \frac{1 + v_1}{\mu}, \tag{28}$$

where $v(p)$ is the relative variance of the photoelectrons transfer efficiency.

Fitting the data using eq. (28) with v_1 fixed, we obtained $v(p) = 8.7 \cdot 10^{-3}$. This is a too small value to influence the estimation of small μ, but it becomes noticeable for a bigger μ.

In table 6, we show recalculated values for the $\mu \geq 1$. These are also found in table 2, in the 6th column.

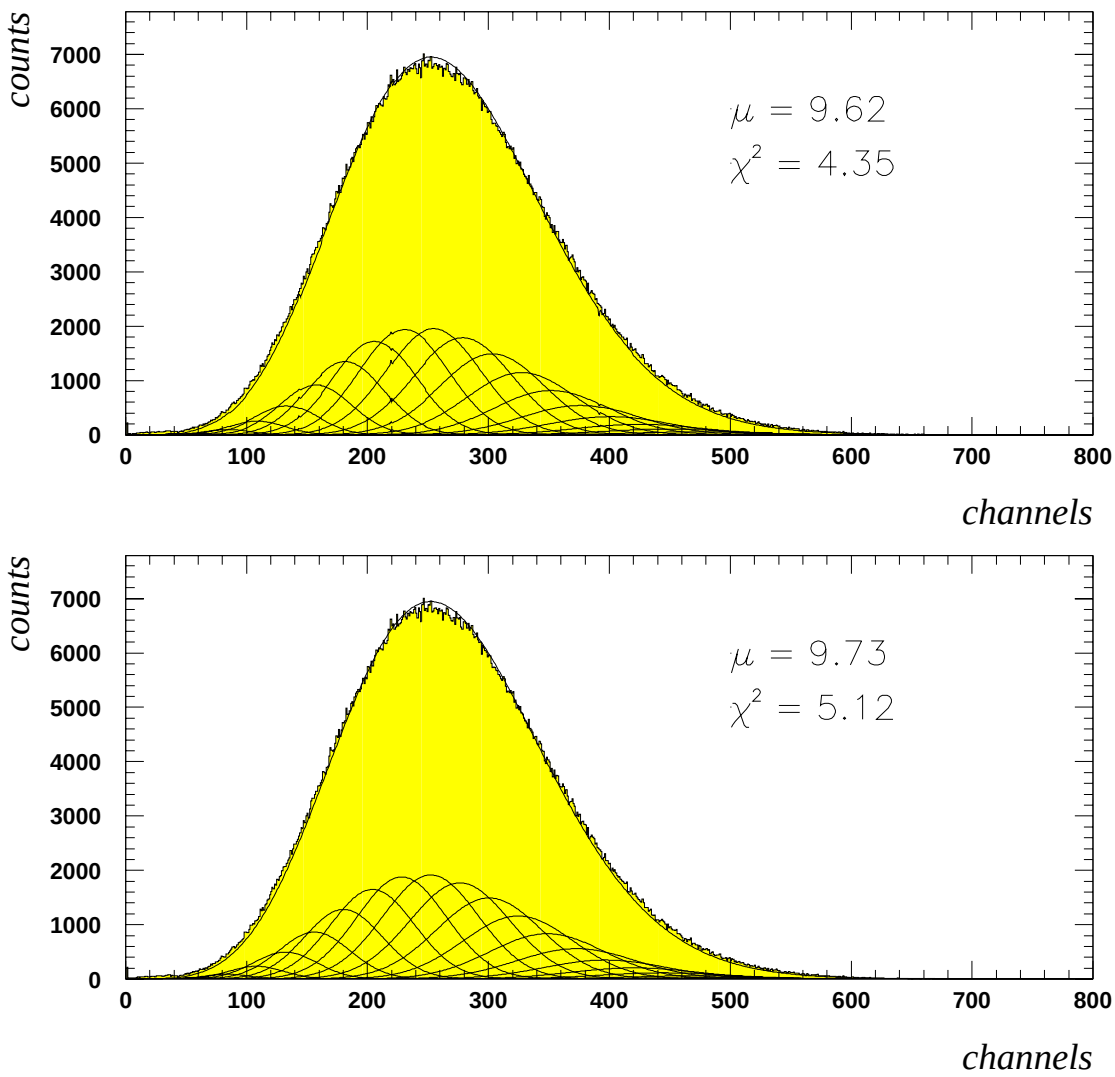

Figure 8: *PMT charge spectrum fit using the convolution method (upper plot) and the gaussian approximation for the fitting functions.*

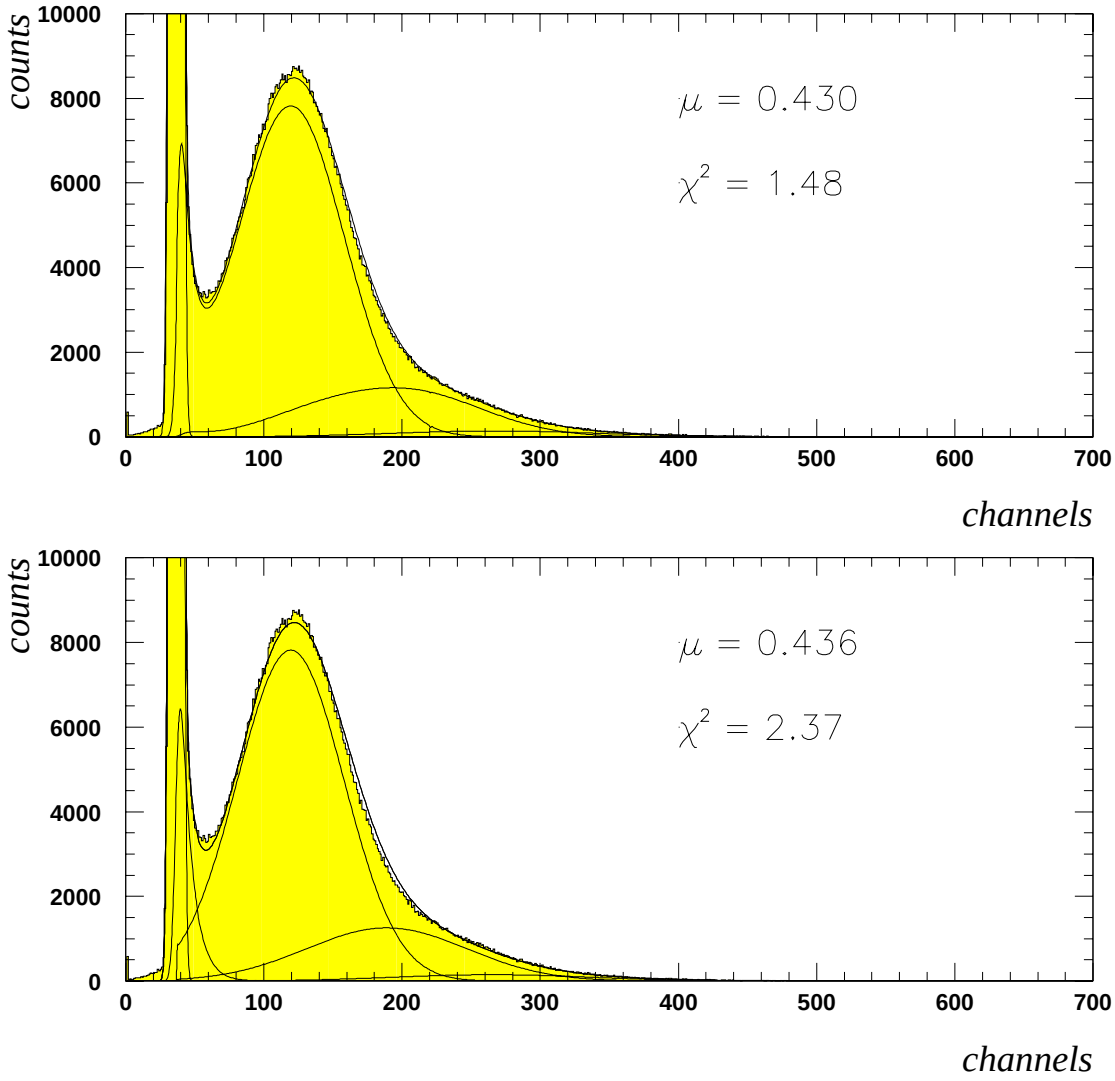

Figure 9: *PMT charge spectrum fit using the convolution method (upper plot) and the combined gaussian one.*

Table 6: Recalculated values for the relative variance method.

$\mu = x_m/x_1$	$\mu = (v_1+1)/v$	$\mu = (1+v_1)/(v-v(p))$
1.10	1.08	1.09
2.12	2.06	2.10
4.16	3.99	4.20
10.2	9.46	10.2
21.7	18.8	21.7

Table 7: Recalculated values for the relative variance method.

N_0	μ_I	μ_F	χ^2	$v(p)(10^{-3})$
1	21.7	21.8	1.65	4.7
2	10.2	10.2	2.14	7.6
3	4.16	4.20	1.70	7.0

5.8 Fit correction for the electrons transfer fluctuations

The effect of the electrons transfer fluctuation should also be taken into account for the proper fitting of the PMT charge distribution for large μ. Indeed, fitting the charge distribution with $\mu \simeq 10$ using the gaussian approximation the σ of the fitting curve tends to be slightly less than the experimental value (see figure 10).

Fluctuations in the transfer efficiency will lead finally to increase the distribution spread. In order to account for this we introduce the additional parameter $v(p)$ [1]:

$$\sigma_N^2 = N(\sigma_1^2 + \mu x_1^2 v_p) + \sigma_p^2. \tag{29}$$

We implemente the fit using eq. (29) for charge distributions with $\mu > 4$. In table 7, where the fitting results are presented, one can see that $v(p) \sim 7 \cdot 10^{-3}$.

An example of the fit is presented in the figure 11, the quality of the fit is better, though the μ values remains almost unchanged. This is a consequence of the Poisson character of the primary electrons counting, which is the main assumption in the fitting function. The last column of table 7 reports the results obtained with such correction.

[1] It is easy to check that the same distribution spread will provide the use of the following formulae:

$$\sigma_N^2 = N(\sigma_1^2 + (N-1)x_1^2 v_p) + \sigma_p^2. \tag{29a}$$

$$\sigma_N^2 = N\sigma_1^2 + \mu^2 x_1^2 v_p + \sigma_p^2. \tag{29b}$$

The formula (29) has been chosen after the analysis of the fit quality (see 5.6)

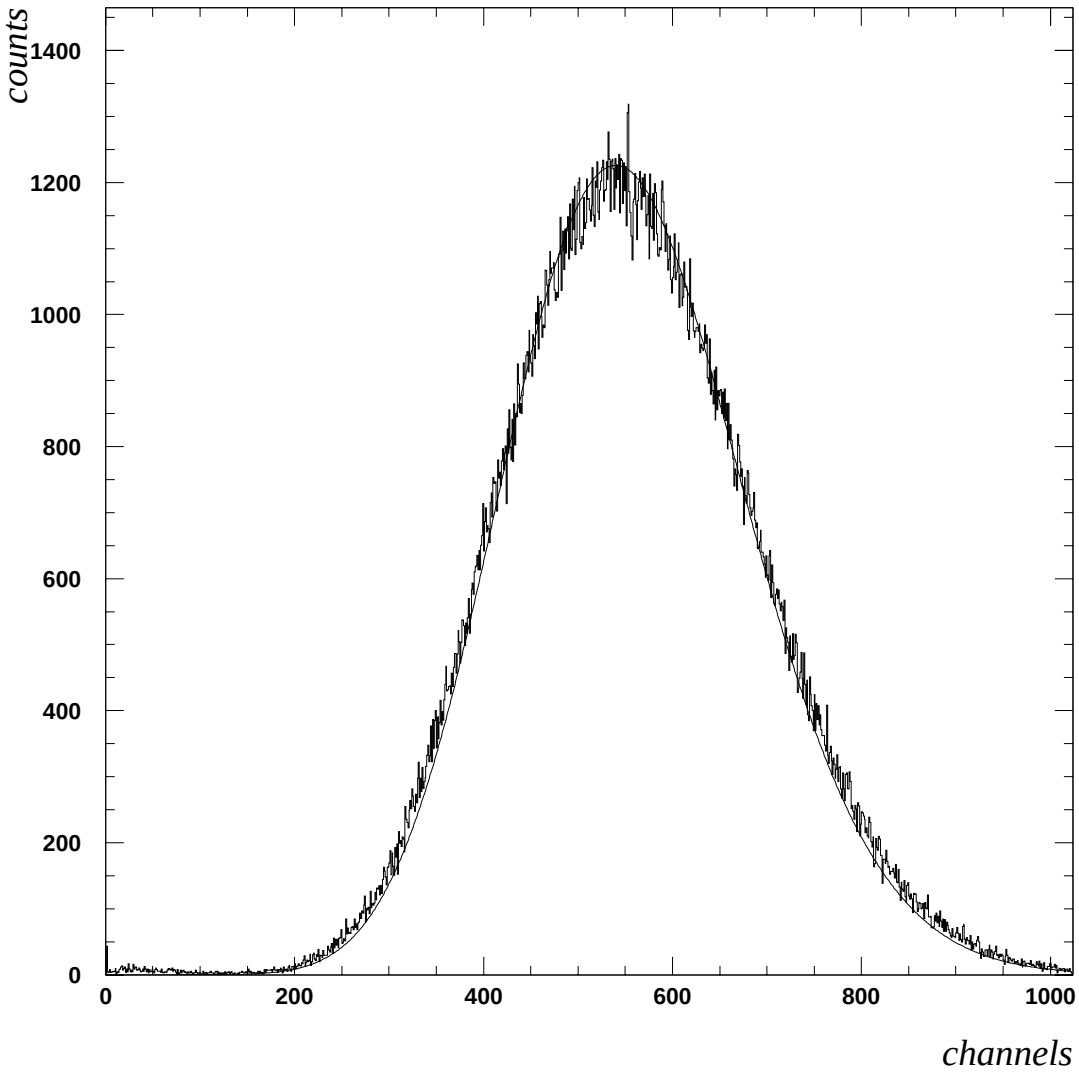

Figure 10: PMT charge spectrum fit using the gaussian approximation. The mean number of p.e. is calculated to be 21.71 and χ^2=2.76.

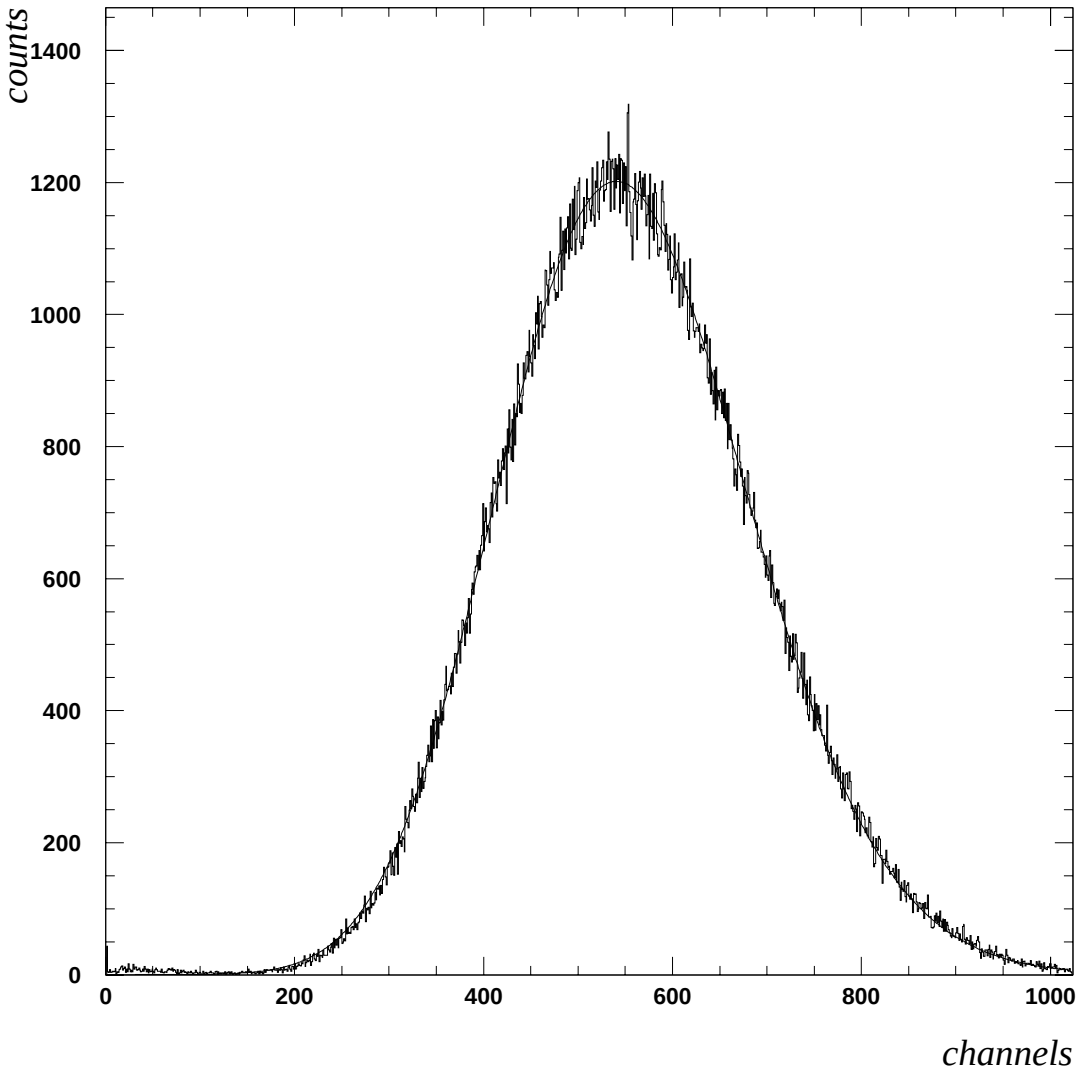

Figure 11: PMT charge spectrum fit with correction for the light transfer fluctuations. The mean p.e. number is 21.68 and χ^2=1.80.

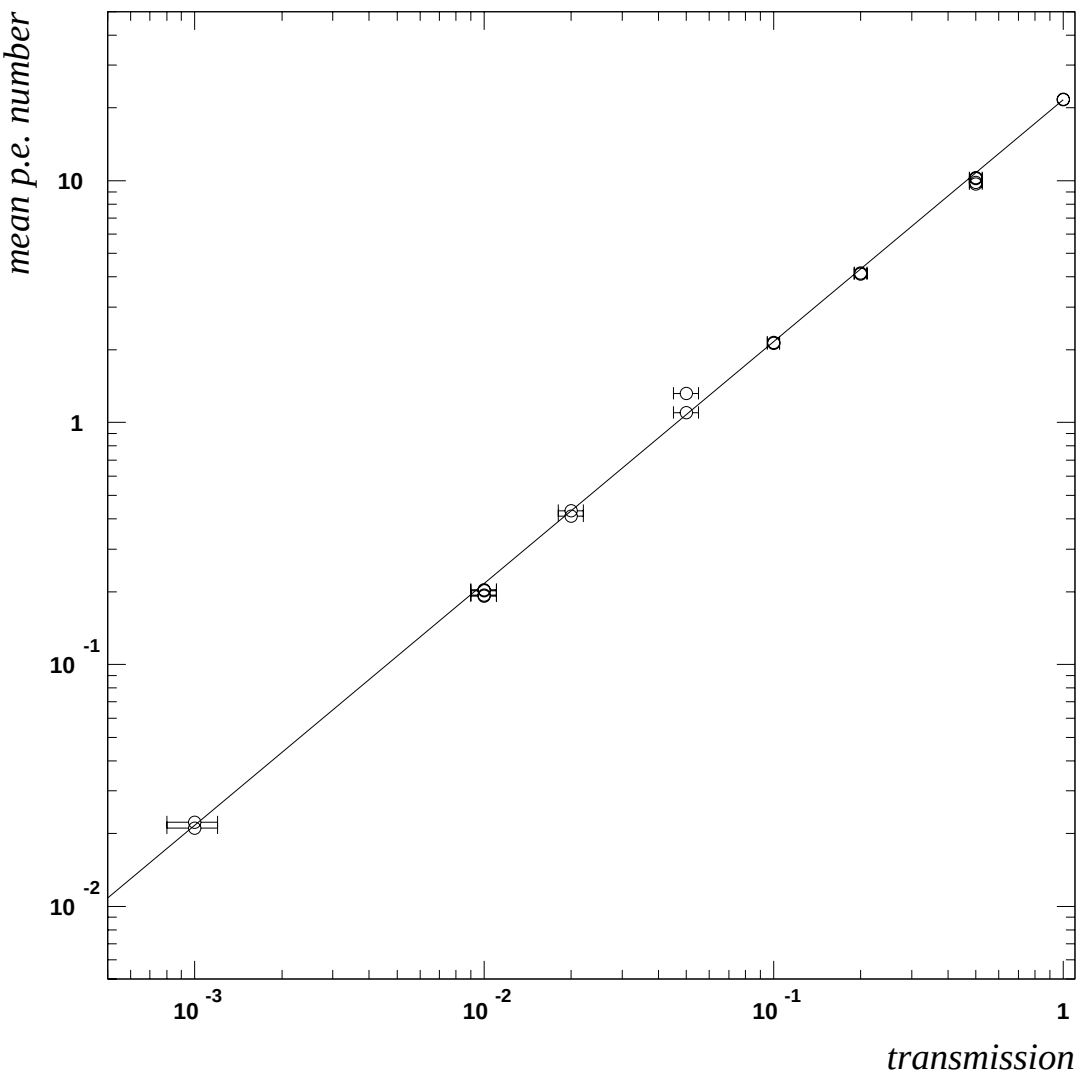

Figure 12: Calculated mean p.e. number (x_m/x_1) vs declared transmission as reported in table 1

6 Conclusions

The assumption of the Poisson distribution of the detected p.e. number proved to be reasonable for our experimental conditions, as well as the model chosen for the SER. In figure 12, we presente a logarithmic plot where the estimated p.e. number is shown as dependence on the transmittancy of the filters.

All of the methods give values which are in a good agreement with expected linear dependence of the p.e. number registered on the filter transparency. The figure demonstrates the linearity of the setup in the dynamic range of 0.02-20 p.e.

The best method for p.e. number estimation in the $0.2 < \mu < 5$ range in an experimental conditions (when the variations of the light transfer efficiency are bigger then in the laboratory set-up) is the fit of the PMT charge distribution with the function (A6) of appendix A with x_0,σ_0,p_E and A values fixed to the values found during the independent PMT calibration and with free μ and $v(p)$.

The advantage of the fitting method is its ability to restore μ from "cut" charge distribution. In the case where the independent calibration was not performed the functions of appendix A can be used with free parameters in order to estimate x_1 (using Appendix A formula). This will need more statistics.

If the charge distribution has "no cut" and the SER (or x_1 parameter) is known, the mean p.e. number can be estimated by dividing the mean of the distribution by the calibration value x_1(position of the mean for a "pure" SER).

7 Acknowledgments

We would like to thank the I.N.F.N. for supporting this work, Roberto Scardaoni and Francesco Sacchetti from I.N.F.N. Milan, Albert Sotnikov from J.I.N.R. for their contribution in constructing the experimental set-up and F. Hartmann for the careful reading of manuscript.

References

[1] J. Veloso and C.A.N. Conde, IEEE Transaction on Nuclear Science, Vol. 40 (1993).

[2] A.G. Wright, IEEE Transaction on Nuclear Science, Vol.34, No.1, February 1987.

[3] A.G. Wright THORN EMI Electron Tubes Limited, Photodetection Information Service *Source of noise in photomultipliers.*

[4] B.H. Candy Rev. Sci. Instrum. 56(2), 1985.

[5] P.B. Coates J. Phys. D: App. Phys., Vol. 6, 1973.

[6] J.B. Birks, The Theory and Practice of Scintillation Counting, Pergamon Press.

[7] E.H. Bellamy et al. NIM A339(1994) 468-476

[8] V. Cavasinni et al. ATLAS Internal Note TILECAL-NO-117

[9] Photomultiplier tubes principles and applications, Philips

[10] BOREXINO Collaboration, Ultra-low measurements in a large volume underground detector, Astroparticle Physics 8(1998) 141-157.

[11] BOREXINO Collaboration, Phys. Lett. B, 422(1998)349

A APPENDIX: Function for the PMT response fitting for the $\mu \simeq 1$

Formula (14) cannot be implemented to fit the PMT response to a light source with intensity of $\simeq 1$ p.e. because of the approximate character of the estimation of x_1 and σ_1. These quantities can be estimated precisely in our model as:

$$x_1 = \left(x_0 + \frac{\sigma_0}{\sqrt{2\pi} g_N} exp\left(-\frac{1}{2}\left(\frac{x_0}{\sigma_0}\right)^2 \right) \right)(1 - p_E) + p_E \cdot A \qquad (A1)$$

$$\sigma_1^2 = \left(x_0^2 + \sigma_0^2 + \frac{x_0 \sigma_0}{\sqrt{2\pi} g_N} exp\left(-\frac{1}{2}\left(\frac{x_0}{\sigma_0}\right)^2 \right) \right)(1 - p_E) + 2p_E \cdot A^2 - x_1^2 \qquad (A2)$$

where p_G is a normalization factor taking into account the cut of the gaussian part of the SER spectra:

$$g_N = \frac{1}{2}\left(1 - erf\left(-\frac{x_0}{\sqrt{2}\sigma_0} \right) \right) \qquad (A3)$$

Another problem arises from the substitution of the multiple p.e. responses with gaussians. While for $n \geq 3$ the gaussian is a very good approximation (see fig.5), there is a significant deviation from the gaussian shape in the n=2 response. Precise analytical formula for the $f_1 \otimes f_2$ convolution is quit complicated and its use in the fitting procedure slows down the calculation. The following approximation can be obtained neglecting the smallest contributions (x should be replaced by $x - x_p$ in the right part of the equation in the case of non-zero pedestal value):

$$f_2(x) = {p_E}^2 \frac{x}{A^2} e^{-\frac{x}{A}} + 2\frac{(1 - p_E)p_E}{\sqrt{2\pi}\sigma_0} exp\left(-\frac{1}{2}\left(\frac{x - x_0 - A}{\sigma_0} \right)^2 \right) +$$

$$+ \frac{(1 - p_E)^2}{2\sqrt{\pi}\sigma_0} exp\left(-\frac{1}{2}\left(\frac{x - 2x_0}{\sigma_0\sqrt{2}} \right)^2 \right) \qquad (A4)$$

The last problem of the correct PMT charge spectra fitting is taking into account the photons transfer efficiency v(p) (including all the possible variations of the photocathode

quantum efficiency from point to point and from the angle of incidence etc.) One can neglect this variations only for

$$\mu << \frac{1+v_1}{v(p)} \qquad (A5)$$

For a big enough μ when parameter v(p) is not known it is better to leave it free and use formula (29) for σ_N.

The fitting function for a measured charge spectrum can be written as:

$$f(x) = P(0)f_p(x) + P(1)f_1(x) + P(2)f_2(x) + \sum_{N=3}^{N_{max}} P(N)f_N(x), \qquad (A6)$$

where $P(N)$ is the Poisson distribution and $f_p(x)$ is the noise function. For the functions $f_N(x)$ the gaussian approximation (with parameters defined by (A1) and (A2) is used. $f_1(x)$ function coincides with (8).

The function (A6) has been tested on the C.T.F. (prototype of BOREXINO [10]) data (runs with a Rn source at the center of the detector). It turns out a $\chi^2 \simeq 0.9 - 1.1$ with a statistics of $\simeq 80,000$ events.

The parameter $v(p) \simeq 0.025$ in the C.T.F. is significantly bigger than the one we could expect using our set-up (because of the more complex light transfer in the C.T.F.).

In order to check the stability of the fit 64 samples of 40,000 events each have been acquired using the set-up shown in figure 1 for the same PMT and in the same conditions with $\mu = 2.15$ (defined from the combined statistics with a high precision following the procedure described in 3.2). The fit of each run has been performed. The fit parameters change around their mean values as (for 1σ):

$$< \mu >= 2.151 \pm 0.026;$$
$$< v_1 >= 0.294 \pm 0.014;$$
$$< x_1 >= 244 \pm 2.$$

So we can conclude that a statistics of 40,000 events with $\mu \simeq 2$ is enought to obtain a SER calibration with a 1% precision at the 1σ C.L.

If the SER parameters (x_0,σ_0,p_E and A) are fixed to the values obtained in independent high statistics calibration and only the parameters μ,$v(p)$,x_p and σ_p are free, the fit of the same data samples gives

$$< \mu >= 2.147 \pm 0.009,$$

providing even better estimation of the μ value.

B APPENDIX: The accuracy of the mean p.e. number calculation from the amount of no-p.e. events

The estimation of the mean number of p.e. from the amount of the events in the pedestal is based only on the assumption of the Poisson-like distribution of the p.e. registration

statistics. This means we do not take into account the linearity of the PMT, which is an important point when all the other methods described in this paper but this one are concerned.

However, while implementing this technique, errors can arise in separating small amplitude pulses from pedestal events (no-p.e. events). Here we suppose that pedestal events are separated perfectly.

Let us call P_0 the probability to have a no-p.e. response, then $1-P_0$ is the probability to have a p.e. response. Because of the Poisson law of the registrated p.e.:

$$P_0 = e^{-\mu}. \tag{B1}$$

The mean p.e. number is estimated from:

$$\mu = -ln\left(\frac{N_{ped}}{N_{trigger}}\right). \tag{B2}$$

Therefore, we have a simple binomial law for the probability of having a signal under the pedestal. The mean value and the r.m.s. for this binomial distribution are, respectively:

$$< N_{ped} >= N_{trigger} \cdot P_0, \tag{B3}$$

and

$$\sigma^2_{N_{ped}} = N_{trigger} \cdot P_0 \cdot (1 - P_0). \tag{B4}$$

For a 1σ error estimation we can substitute N_{ped} with $N_{ped} \pm \sqrt{N_{triggers}} e^{-\mu/2}\sqrt{1-e^{-\mu}}$. The error on μ is not symmetrical and it turns out that the bigger error comes out from the substitution of $N_{events} - \sqrt{N_{events}} e^{-\mu/2}\sqrt{1-e^{-\mu}}$. Performing this substitution and taking we have:

$$\mu + \Delta\mu = -ln\left(e^{-\mu} - \frac{1}{\sqrt{N_{trigger}}} e^{-\mu/2}\sqrt{1-e^{-\mu}}\right). \tag{B5}$$

For 1% accuracy at 1σ C.L. $\Delta\mu$=0.01μ and as a consequence

$$N_{trigger} = \frac{1-e^{-\mu}}{e^{-\mu}(1-e^{-0.01\cdot\mu})^2}. \tag{B6}$$

In this way it is possible to work out the number of triggers, $N_{trigger}$. In figure 13 the number of triggers for a 1% accuracy at 1σ C.L. is shown.

C APPENDIX: Corrections to the SER parameters to account for multip.e. hits

Let us consider $P(n)$ as the Poisson distribution of the photoelectrons hitting the first dynode. The mean value of the ADC spectrum will be, supposing the linearity of the

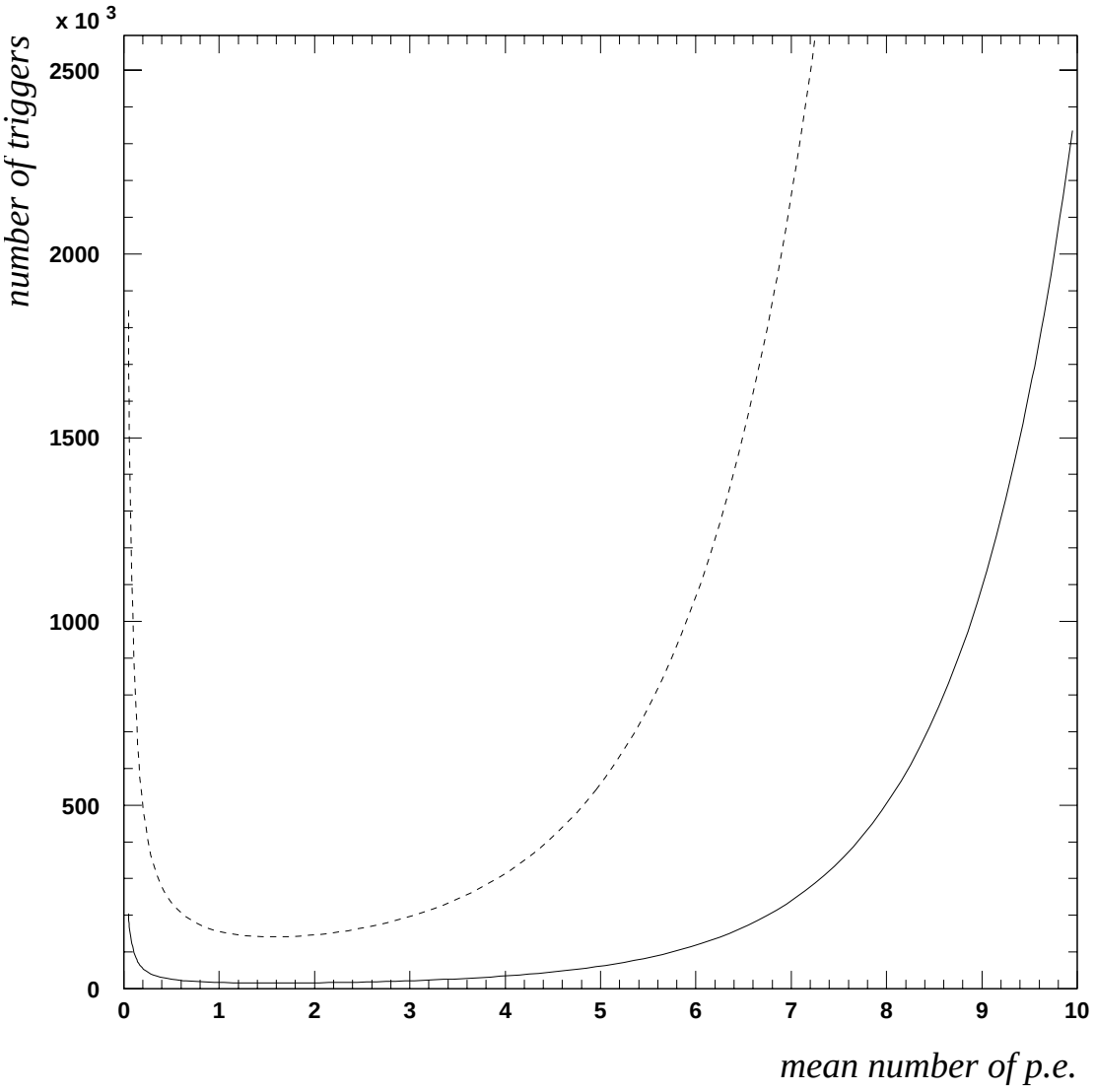

Figure 13: *Statistics for 1% accuracy at 1σ and 3σ C.L. for different mean number of p.e.*

PMT response: $x_n = nx_0$ and $\sigma_n = \sqrt{n}\sigma_0$, where x_0 and σ_0 are respectively the mean value and the standard deviation of the SER; and taking into account the Poissonian distribution of the detected light:

$$x^*_m = \frac{P(0)\cdot 0 + P(1)\cdot x_1 + P(2)\cdot 2x_1 + \ldots}{P(1) + P(2) + \ldots} =$$

$$= x_1 \cdot \frac{\mu}{1 - P(0)}, \qquad (C1)$$

where x_1 is the mean value of the SER and the normalization does not contain P(0) because the pedestal is not measured. When $\mu \ll 1$ the (C1) can be written:

$$x^*_m = \frac{x_1}{1 - \frac{\mu}{2}}. \qquad (C2)$$

To define the relative variance:

$$v^* \equiv \left(\frac{\sigma^*_m}{x^*_m}\right)^2 = \frac{< x^2 >}{< x >^2} - 1. \qquad (C3)$$

one should know $< x^2 >$, where $< x > \equiv x^*_m$:

$$< x^2 > = < x >^2 + (\sigma^*_m)^2 =$$

$$= \frac{P(0)\cdot 0 + P(1)\cdot (x_1^2 + \sigma_1^2) + P(2)\cdot (4x_1^2 + 2\sigma_1^2) + \ldots}{P(1) + P(2) + \ldots} =$$

$$= \frac{\sigma_1 < n > + x_1^2 < n^2 >}{1 - P(0)}, \qquad (C4)$$

where $< n > \equiv \mu$ and $< n > = < n^2 > - < n >^2$ (Poisson distribution) has been used. From (C4) it turns out that:

$$< x^2 > = < n > \cdot \frac{\sigma_1 + (1 + < n >) x_1^2}{1 - P(0)}. \qquad (C5)$$

Therefore the relation between v^* and v_1 is:

$$v^* = (v_1 + 1) \cdot \frac{1 - e^{-\mu}}{\mu} - e^{-\mu}. \qquad (C6)$$

For $\mu \ll 1$ (C6) becomes:

$$v^* = v_1\left(1 - \frac{\mu}{2}\right) + \frac{\mu}{2}. \qquad (C7)$$